

## Mechanical Properties of 3D-Printed PETG Samples: The Effect of Varying Infill Patterns



Osamah Fattah Taresh<sup>1</sup>, Marwan T. Mezher<sup>2\*</sup>, Entihaa G. Daway<sup>3</sup>

<sup>1</sup> Institute of Technology, Middle Technical University, Baghdad 10074, Iraq

<sup>2</sup> Institute of Applied Arts, Middle Technical University, Baghdad 10074, Iraq

<sup>3</sup> Engineering Technical College, Middle Technical University, Baghdad 10074, Iraq

Corresponding Author Email: [marwantahir90@gmail.com](mailto:marwantahir90@gmail.com)

<https://doi.org/10.18280/rcma.330508>

### ABSTRACT

**Received:** 7 September 2023

**Revised:** 20 September 2023

**Accepted:** 10 October 2023

**Available online:** 31 October 2023

#### Keywords:

*additive manufacturing, fused deposition modeling (FDM), polyethylene terephthalate glycol (PETG), infill patterns, mechanical properties*

One of the most cost-effective additive manufacturing (AM)/3D printing techniques for complicated geometry components is fused deposition modeling (FDM). FDM is a method of fabricating parts by depositing successive layers of material in accordance with computer-aided design file. The properties of the finished products manufactured with FDM are sensitive to the process parameters used. Most FDM items still lack adequate mechanical characteristics when compared to those produced using conventional methods. This investigation seeks to address this knowledge gap by fabricating tensile specimens from Polyethylene Terephthalate Glycol (PETG) filament in a variety of geometries, including grids, octets, triangles, and hexagons. To verify this claim, samples studied was printed with varying infill percentages (25, 50, 75, and 100) % to see how this impacted the mechanical characteristics such as tensile strength and fractured strain. Although the best results for tensile stress and hardness were achieved with a 100% infill percentage in all four printing situations, the triangles orientation consistently produced the best results.

## 1. INTRODUCTION

The development and widespread use of additive manufacturing (AM) methods like 3D printing in recent years may be attributed to the technologies' adaptability, speed of reaction, and cheap cost [1]. The construction, medical, robotic, military, automotive, and aerospace sectors [1-15], to name a few, have all benefited from this technology. Moreover, AM offers benefits like reduced manufacturing costs and a means by which manufacturers may tailor low-volume items to individual customers' preferences in a cost-effective and expedited manner [16, 17]. Less expensive materials, molds, and dies may be used thanks to applications of the AM process. With this method, businesses or individuals may save money while still trying out new ideas [18, 19].

The ability of AM technology to reduce the carbon footprint of manufacturing is another area in which it excels. This is accomplished through the use of fewer raw materials, the generation of less waste material, the creation of reduced-weight parts with enhanced specifications, and the production of parts on demand. One kind of additive manufacturing (AM) that uses material extrusion is called fused deposition modeling (FDM). It is the most widely used AM technology in both the home and industrial settings, and it is also one of the most quickly developing AM processes. AM of metal components involves heating, melting, solidifying, and cooling metal alloys with spatially varying temperatures over the whole part. Relying upon the product thermo-physical characteristics, the stiffness of the component, and the transient temperature fields, localized portions of a part may undergo permanent deformation [20].

The sensitivity of different alloys to deformation and the associated dimensional inaccuracy of the final product may be evaluated quantitatively using a suitable model for the estimate of strain. Several studies in recent years have focused on optimizing the mechanical qualities of 3D printed components. Given that the properties of the printed items might be affected by a wide variety of process-level factors. The effect of deposition direction on the functionality of FDM parts has been analyzed and discussed by Casavola et al. [21] and Domingo-Espin et al. [22] through manufacturing samples with different orientations and analyzing the mechanical properties of the printed samples. Research on other parameters, such as raster angle [23], plate temperature [24] layer-to-layer thickness [25], and types of structure [26], has also been completed. The surface quality and mechanical strength of printed ABS specimens were studied by Vargas and Cordoba [27], who looked into the impact of the extrusion speed and the deposition distance on the process. Ultimate strength of 49 MPa and Young modulus of 1893 MPa were achieved with no degradation observed of the specimens' outer surfaces.

The FDM approach was investigated by Tymrak et al. [28] using low-cost commercial ReoRap printers to print ABS and PLA. Layer thicknesses ranging from 0.2 to 0.4 mm, angle variations between +45° and -45°, from 0° to 90°, and a speed equal 5 mm/min were the parameters used in fabrication. Maximum stress results for PLA were 33.68MPa and for ABS was 56.6MPa. Fill density values from 0% to 100% and the filling pattern were utilized as production factors by Guamantario [29]. The filling pattern was one of two typically employed in printing processes. The test findings revealed that

the mechanical strength of 3D printed items was affected by the density and fill pattern used in the printing process. Most importantly, the properties of additively manufactured components using 3D printing technique are affected by the filling factor, print and raster direction, and layer-to-layer thickness [30]. There is a great deal of studies [31-49] analyzing the effect of various variables on mechanical characteristics, especially tensile characteristics. Camposeco-Negrete [50] analysed the impact of layer print size, infill shape, raster direction of 3D-printed parts using Taguchi and ANOVA methods. The outcomes referred to that the printing plane the most influential factor on tensile and yield strength, and dimensional accuracy of thickness printed parts. Zhao et al. [51] studied the mechanical properties of PLA printed components by altering the deposition layer size and raster angle and. Tensile strength enhanced when using higher printing angle. The purpose of the study investigated by Verbeeten et al. [52] was to analyse the effect of the printing speed and infill orientation angle on the strain-rate dependence of for the tensile 3D-printed PLA samples. They concluded that changing the filling angle resulted in anisotropic effects to the samples. Hassanifard and Hashemi [53] investigated the strain-life fatigue through analyse the impact of printing angle and direction of PC and PLA printed components. The researchers stated that the filling density impacted the mechanical characteristics of the manufactured samples.

From analysis the above studies, there is no such paper has analysed the infill patterns effect of the PETG printed samples on the mechanical properties. Therefore, this study aims to investigate how adjusting certain parameters of the fused deposition modeling process affects the mechanical properties of 3D-printed PETG. The specimens were printed with varying infill percentages and geometric forms so that the effect of the print configuration parameter could be examined. Several configurations and infill percentages were employed to examine the mechanical characteristics of the printed components, and the tensile and hardness results were analyzed accordingly.

## 2. MATERIALS AND METHODS

### 2.1 Materials

Polyethylene Terephthalate Glycol (PETG) filament with a 1.75 mm diameter was employed with the 3D printing machine in the present work. The filament wire was heated and extruded in accordance with the layer-to-layer to manufacturing the 3D printing samples. PETG is a vastly known 3D printing filament, greatly employed due its good strength, relative flexibility, and temperature resistance in contrast with the PLA. PETG provides the strength of ABS parts with even more flexibility. It is perfect for practical prints that require a little elasticity property prior to breaking than PLA. Consequently, it displaced ABS as the second most popular 3D printing filament on the market.

### 2.2 Methods

The experiment specimens were manufactured utilizing the ANYCUBIC commercial 3D printer and the Fused Deposition Modeling (FDM) method, Figure 1 presents the 3D printer that used in the present work. The diameter of this printer's nozzle is 0.4 millimeters. The tensile test samples were 3D printed

using Polyethylene Terephthalate Glycol (PETG) filament with a 1.75 mm diameter. Four tensile samples of each configuration (grid, octet, triangle, and hexagon) were printed with four different infill percentages (25%, 50%, 75%, and 100%). As can be seen in Figure 1, the printed specimen was constructed using the D638 type IV sample because this design is practical for the uses of the polymer material that are consistent with the study [38]. The sample's 3D CAD model was created in Solidworks 2020 and exported as a ".STL" file. The STL file (3D model) was used with the Ultimaker Cura 4.3 software for slicing. G-code is the file type that may be used by the 3D printer once it has been exported from the slicing program. The printing temperature was kept at 195°C, while the platform temperature was kept at 60°C. Printing settings also included a print speed of 50 mm/s, a wall thickness of 0.15 mm and a layer height of 0.1 mm. Figure 2 shows the 3D-printed tensile samples. Table 1 shows the 3D-printer experimental parameters used in the current study.

**Table 1.** The printing parameters of the different printing patterns

| Infill Pattern   | Infill Percentage % |
|------------------|---------------------|
| <b>Grids</b>     | 25, 50, 75, 100     |
| <b>Triangles</b> | 25, 50, 75, 100     |
| <b>Hexagons</b>  | 25, 50, 75, 100     |
| <b>Octets</b>    | 25, 50, 75, 100     |



**Figure 1.** ANYCUBIC 3D printer



**Figure 2.** Tensile test machine

### 3. RESULTS AND DISCUSSIONS

#### 3.1 Tensile strength

The D638 type IV standard [54] was implemented in order to manufacture the 3D-printed test components, and those samples are shown in Figure 3. The printed specimens from each of the four instances were put through tensile testing on a double-acting hydraulic press that had a maximum loading capacity of 30 tons. This testing allowed the tensile properties of the specimens to be determined. In order to determine the tensile strength of each identical sample type, three different specimens were evaluated. It was determined that a speed of 5 mm per minute was appropriate for the test. After carrying out a series of tensile tests, the results of which are shown in Figure 4, show the 3D-printed samples under a variety of situations.



Figure 3. The 3D-printed tensile specimens



Figure 4. The fractured 3D-printed tensile specimens

The tensile strength of the PETG samples produced with triangular case and at varying percentages of infill are shown in Figure 5. When the infill percentage was 25%, the tensile strength was found to be 21.12 MPa, which was much lower than the highest value of 31.05 MPa that was recorded when the infill percentage was 100%. The tensile strength of the remaining two infill percentages, which were 50% and 75%, was 23.97 MPa and 24.23 MPa, respectively. As can be seen in Figure 6, the tensile strength of the grid case rose when the percentage of the material that was filled in was raised. In Figure 6, It can be seen how the tensile strength values of the grid case change depending on the percentage of infill that is used. There is no denying that an increase in the filling percentages will lead to an increase in the tensile strength. The grid case had a tensile strength of 27.05 MPa when it had

100% infill percentage, however the result was only 21.06 MPa when it had 25% filling percentage. The relationship between the tensile strength and the filling percentages of the hexagonal case is shown in Figure 7, which may be seen here. The tensile strength was improved by incrementing the infill percentage, and the greatest value of 24.56 MPa was obtained when the infill percentage was 100%, whilst the lowest value of 18.15 MPa was recorded when the infill percentage was 25%. With reference to Figure 8, which illustrates the impact of the infill rate on the tensile strength values of the octet case, showing that the tensile strength improves with rising the filling rate. The tensile strength of the material was measured to be at its highest level of 24.12 MPa when it included an infill percentage of 100%. On the other hand, the value was found to be at its lowest level when it contained just 25% of the total volume.

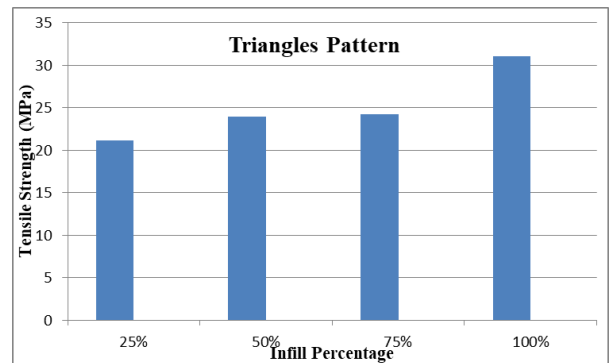


Figure 5. Impact of the infill percentage on the tensile strength of the triangle case

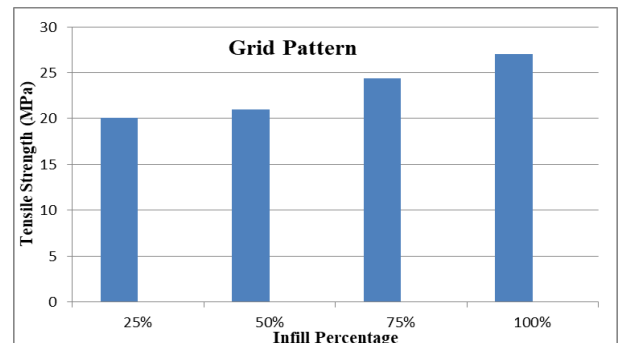


Figure 6. Tensile strength of the grid case with various percentage

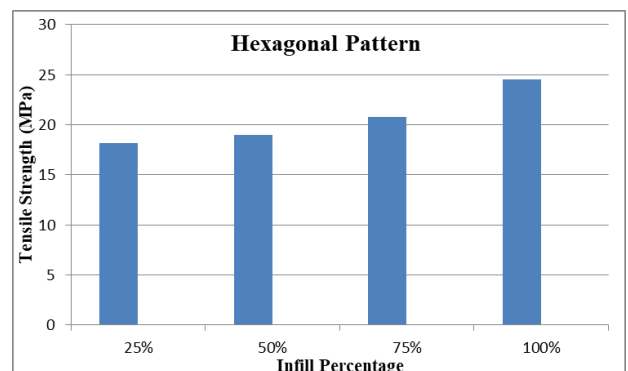
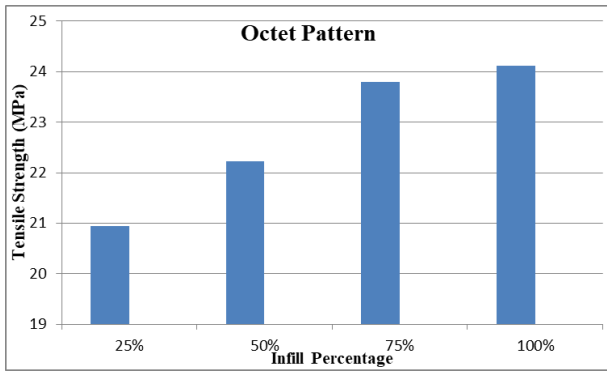


Figure 7. Impact of the infill percentage on the tensile strength of the hexagonal case



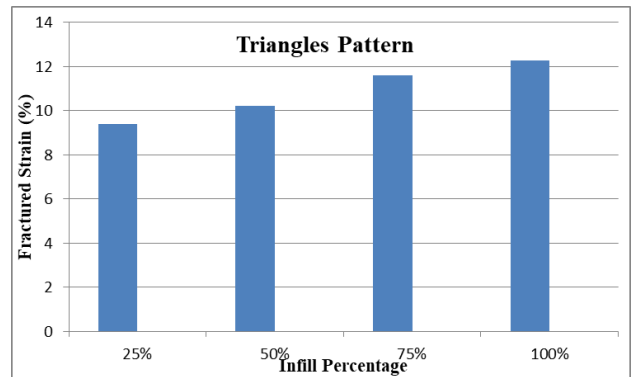
**Figure 8.** Impact of the infill percentage on the tensile strength of the octet case

Increasing the tensile strength of the 3D-printed components that occurs in conjunction with an increase in the filling percentage is attributable to an increase in the volume of the printing material that is present within the internal structure of the samples. Increasing the filling percentage causes more layers to be produced in the internal structure. This causes the samples to endure more plastic strain before they fracture, which in turn increases their tensile strength. Consequently, it can be referred that the resulting tensile strength increases with increasing the infill percentage for all 3D printed geometric shapes, this attributable to the increment in the sample stiffness and lowering in its susceptibility distortion.

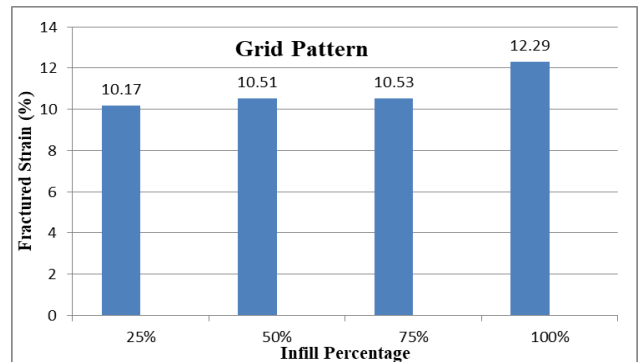
### 3.2 Fractured strain

Figure 9 illustrates how the percentage of infill affects the fractured strain in the 3D-printed samples used for the triangle case study. It was evident from the results that an increase in the filling factor led to an increase in the fractured strain. It was discovered that the greatest fractured strain was 12.27%, which was recorded with a percentage of infill equal to 100%, while the 25% filling factor leads to a fractured strain of 9.39%. Figure 10 depicts the impact that the infill percentage of the grid printing case has on the grid printing case. When the filling factor was adjusted to 25%, the fractured strain was only 10.17%, but when the filling factor was increased to 100%, the final strain was 12.29%. This shows that the fractured strain grows as the filling factor increases. Figure 11 presents a comparison of the filling percentage of the hexagonal filling pattern with the other filling patterns. The findings revealed that an increase in the filling ratio is associated with an increase in the fractured strain. As can be observed in Figure 10, the greatest cracked strain that was recorded was 9.11%, and this was achieved when the filling percentage was 100%. The minimum number was 4.89%, while the infill percentage was set at 25%. Figure 12 depicts the shifts that take place in the fractured strain of the octet pattern case as a function of the different infill percentages. The fractured strain had the maximum value when it was equal to 14.26% when the filling factor was equal to 100%, while it had the lowest value when it was equal to 12.67% when the filling percentage was equal to 25%. The improvement in the fractured strain with increasing the filling factor of all printing cases is due to increase the strength of the internal structure of the 3D-printed components and this resulted in increasing the samples durability when its subjected tensile loading and thus the fractured strain of the samples with higher infill percentage

was higher than those with lower filling percentages.



**Figure 9.** Variation in the fractured strain with the infill percentage of the triangle case



**Figure 10.** Variation in the fractured strain with the infill percentage of the grid case

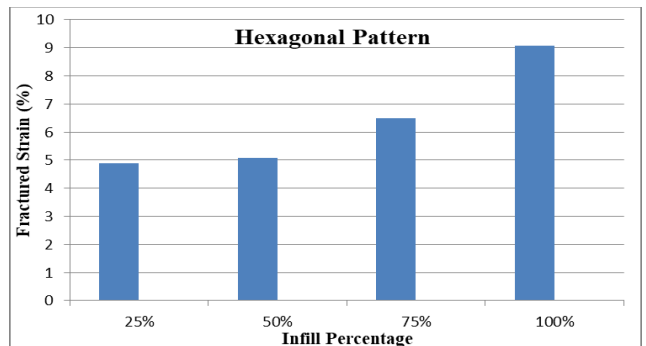


**Figure 11.** Variation in the fractured strain with the infill percentage of the hexagonal case

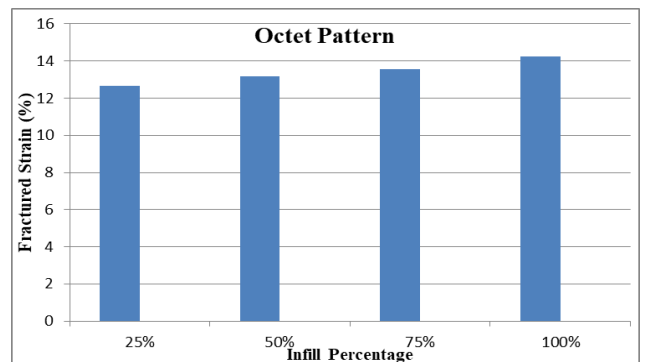


**Figure 12.** Variation in the fractured strain with the infill percentage of the octet case

#### 4. CONCLUSIONS

This article investigates the FDM 3D printing product's mechanical properties. In this study, we used a filament made of polyethylene terephthalate glycol (PETG). Several infill percentages were used to print tensile specimens in a wide variety of 3D-printing patterns, including grids, octets, triangles, and hexagons. The following are inferences that may be drawn from the data:

1. The tensile strength and fractured strain findings vary significantly depending on the filling pattern and infill percentage.

2. The 3D-printed samples with the greatest tensile strength were those filled with triangles, while the ones with the lowest value were those filled with octets.

3. The tensile strength of all four filling patterns increased when the filling percentage was raised.

4. The octet case exhibited the greatest fractured strain, while the hexagonal filling pattern showed the lowest.

5. The commercial FDM 3D printers might be used as a cost-effective and high-quality option for manufacturing components with exact dimensions and great precision.

#### REFERENCES

- [1] Maidin, S., Muhamad, M.K., Pei, E. (2015). Feasibility study of ultrasonic frequency application on FDM to improve parts surface finish. *Journal Teknologi*, 77(32): 27-35. <https://doi.org/10.11113/jt.v77.6983>
- [2] Concli, F., Molinaro, M. (2023). Design for additive manufacturing: cost evaluations. *International Journal of Computational Methods and Experimental Measurements*, 11(1): 1-8. <https://doi.org/10.18280/ijcmem.110101>
- [3] Wang, G., Cheng, T., Do, Y., Yang, H., Tao, Y., Gu, J., An, B., Yao, L. (2018). Printed paper actuator. in *Proceedings of the 2018 CHI Conference on Human Factors in Computing Systems - CHI '18*, pp. 1-12. <https://doi.org/10.1145/3173574.3174143>
- [4] Concli, F., Molinaro, M. (2022). Design for additive manufacturing – material characterization and geometrical optimization. *International Journal of Computational Methods and Experimental Measurements*, 10(2): 146-157. <https://doi.org/10.2495/CMEM-V10-N2-146-157>
- [5] Fu, J., Yu, X., Jin, Y. (2018). 3D printing of vaginal rings with personalized shapes for controlled release of progesterone. *International Journal of Pharmaceutics*, 539(1-2): 75-82. <https://doi.org/10.1016/j.ijpharm.2018.01.036>
- [6] Pant, M., Pidge, P., Nagdeve, L., Kumar, H. (2021). A review of additive manufacturing in aerospace application. *Revue des Composites et des Matériaux Avancés-Journal of Composite and Advanced Materials*, 31(2): 109-115. <https://doi.org/10.18280/rcma.310206>
- [7] Bustillo, J.P., Tumlos, R. Remoto, R.Z. (2019). Intensity modulated radiotherapy (IMRT) phantom fabrication using fused deposition modeling (FDM) 3D printing technique. *Biomedizinische Technik/Biomedical Engineering*, 27(10): 509-515. [https://doi.org/10.1007/978-981-10-9023-3\\_92](https://doi.org/10.1007/978-981-10-9023-3_92)
- [8] Alshwairekh, A.M. (2023). A computational fluid dynamics study on polymer heat exchangers for low-temperature applications: Assessing additive manufacturing and thermal-hydraulic performance. *International Journal of Heat and Technology*, 41(3): 602-610. <https://doi.org/10.18280/ijht.410312>
- [9] Hua, D., Zhang, X., Ji, Z., Yan, C., Yu, B., Li, Y., Wang, X., Zhou, F. (2018). 3D printing of shape changing composites for constructing flexible paper-based photothermal bilayer actuators. *Journal of Materials Chemistry C*, 6(8): 2123-2131. <https://doi.org/10.1039/C7TC05710E>
- [10] Ali, H.B., Oleiwi, J.K., Othman, F.M. (2022). Compressive and tensile properties of ABS material as a function of 3D printing process parameters. *Revue des Composites et des Matériaux Avancés-Journal of Composite and Advanced Materials*, 32(3): 117-123. <https://doi.org/10.18280/rcma.320302>
- [11] Esposito, C.C., Palumbo, E., Masciullo, A., Montagna, F., Torricelli, M.C. (2018). Fused deposition modeling (FDM): An innovative technique aimed at reusing Lecce stone waste for industrial design and building applications. *Construction and Building Materials*, 158: 276-284. <https://doi.org/10.1016/j.conbuildmat.2017.10.011>
- [12] Ikubanni, P.P., Adeleke, A.A., Agboola, O.O., Christopher, C.T., Ademola, B.S., Okonkwo, J., Adesina, O.S., Omoniyi, P.O., Akinlabi, E.T. (2022). Present and future impacts of Computer-Aided Design/ Computer-Aided Manufacturing (CAD/CAM). *Journal Européen des Systèmes Automatisés*, 55(3): 349-357. <https://doi.org/10.18280/jesa.550307>
- [13] Mauduit, A., Gransac, H., Pillot, S. (2021). Influence of the manufacturing parameters in selective laser melting on properties of aluminum alloy AlSi7Mg0.6 (A357). *Annales de Chimie - Science des Matériaux*, 45(1): 1-10. <https://doi.org/10.18280/acsm.450101>
- [14] Gioumouxouzis, C.I., Katsamenis, O.L., Bouropoulos, N., Fatouros, D.G. (2017). 3D printed oral solid dosage forms containing hydrochlorothiazide for controlled drug delivery. *Journal of Drug Delivery Science and Technology*, 40: 164-171. <https://doi.org/10.1016/j.jddst.2017.06.008>
- [15] Vaidya, M., Arulmozhi, R.S., Anuraag, K., Ashok, D.K., Poojalakshmi, M.G. (2018). 3D design and printing of custom-fit finger splint. *Biomedical Engineering Applications Basis and Communications*, 30(5): 1850032. <https://doi.org/10.4015/S1016237218500321>
- [16] Schmitt, M., Mehta, R.M., Kim, I.Y. (2020). Additive manufacturing infill optimization for automotive 3Dprinted ABS components. *Rapid Prototyping Journal*, 26(1): 89-99. <https://doi.org/10.1108/RPJ-01-2019-0007>
- [17] Chen, N., Frank, M. (2019). Process planning for hybrid additive and subtractive manufacturing to integrate machining and directed energy deposition. *Procedia Manufacturing*, 34: 205-215. <https://doi.org/10.1016/j.promfg.2019.06.140>
- [18] Bual, G.S. (2014). Methods to improve surface finish of parts produced by fused deposition modeling. *Manufacturing Science and Technology*, 2(3): 51-55. <https://doi.org/10.13189/mst.2014.020301>
- [19] Patel, R., Patel, S., Patel, J. (2014). A review on optimization of process parameter of fused deposition modeling for better dimensional accuracy. *International Journal of Engineering Development and Research*, 2(2): 1620-1624.

- [20] Gibson, I., Rosen, D., Stucker, B. (2015). Additive manufacturing technologies: 3D printing, rapid prototyping and direct digital manufacturing. <https://doi.org/10.1007/978-1-4939-2113-3>
- [21] Casavola, C., Cazzato, A., Moramarco, V., Pappalettere, C. (2016). Orthotropic mechanical properties of fused deposition modelling parts described by classical laminate theory, *Materials & Design*, 90: 453-458. <https://doi.org/10.1016/j.matdes.2015.11.009>
- [22] Domingo-Espin, M., Puigoriol-Forcada, J.M., Garcia-Granada, A.A., Llumà, J., Borros, S., Reyes, G. (2015). Mechanical property characterization and simulation of fused deposition modeling polycarbonate parts. *Materials & Design*, 83: 670-677. <https://doi.org/10.1016/j.matdes.2015.06.074>
- [23] Ning, F., Cong, W., Hu, Y., Wang, H. (2017). Additive manufacturing of carbon fiber-reinforced plastic composites using fused deposition modeling: Effects of process parameters on tensile properties. *Journal of Composite Materials*, 28(4): 451-462. <https://doi.org/10.1177/0021998316646169>
- [24] Wang, L., Gardner, D.J. (2018). Contribution of printing parameters to the interfacial strength of polylactic acid (PLA) in material extrusion additive manufacturing. *Progress in Additive Manufacturing*, 3: 165-171. <https://doi.org/10.1007/s40964-018-0041-7>
- [25] Sood, A.K., Ohdar, R.K., Mahapatra, S.S. (2010). Parametric appraisal of mechanical property of fused deposition modelling processed parts. *Materials & Design*, 31(1): 287-295. <https://doi.org/10.1016/j.matdes.2009.06.016>
- [26] Galeta, T., Raos, P., Stojšić, J., Pakši, I. (2016). Influence of structure on mechanical properties of 3D printed objects. *Procedia Engineering*, 149: 100-104. <https://doi.org/10.1016/j.proeng.2016.06.644>
- [27] Vargas, E., Cordoba, L. (2004). Calidad superficial en el prototipado rápido, proceso FDM. *Revista Ingeniería e Investigación*, 56: 28-32.
- [28] Tymrak, B.M., Kreiger, M., Pearce, J.M. (2014). Mechanical properties of components fabricated with open source 3-D printers under realistic environmental conditions. *Materials & Design*, 58: 242-246. <https://doi.org/10.1016/j.matdes.2014.02.038>
- [29] Guamantario, W.C. (2014). Influencia de los parametros de relleno en el comportamiento mecanico a la flexion de piezas fabricadas en impresoras 3D de bajo coste. *Universitat Politècnica de Valencia*.
- [30] Hanon, M.M., Marczis, R., Zsidai, L. (2019). Anisotropy evaluation of different raster directions, spatial orientations, and fill percentage of 3D printed PETG tensile test specimens. *Key Engineering Materials*, 821: 167-173. <https://doi.org/10.4028/www.scientific.net/KEM.821.167>
- [31] Ayırlımsı, N., Kariz, M., Kwon, J.H., Kuzman, M.K. (2019). Effect of printing layer thickness on water absorption and mechanical properties of 3D-printed wood/PLA composite materials. *The International Journal of Advanced Manufacturing*, 102(5-8): 2195-2200. <https://doi.org/10.1007/s00170-019-03299-9>
- [32] Sood, A.K., Ohdar, R.K., Mahapatra, S.S. (2012). Experimental investigation and empirical modelling of FDM process for compressive strength improvement. *Journal of Advanced Research* 3(1): 81-90. <https://doi.org/10.1016/j.jare.2011.05.001>
- [33] Quan, Z., Suhr, J., Yu, J., Qin, X., Cotton, C., Mirotznik, M., Chou, T.W. (2018). Printing direction dependence of mechanical behavior of additively manufactured 3D preforms and composites. *Composite Structures*, 184: 917-923. <https://doi.org/10.1016/j.compstruct.2017.10.055>
- [34] Crococolo, D., Agostinis M.D., Olmi, G. (2013). Experimental characterization and analytical modelling of the mechanical behaviour of fused deposition processed parts made of ABS-M30. *Computational Materials Science*, 79: 506-518. <https://doi.org/10.1016/j.commatsci.2013.06.041>
- [35] Türk, D.A., Brenni, F., Zogg, M., Meboldt, M. (2017). Mechanical characterization of 3D printed polymers for fiber reinforced polymers processing. *Materials & Design*, 118: 256-265. <https://doi.org/10.1016/j.matdes.2017.01.050>
- [36] Weng, Z., Wang, J., Senthil, T., Wu, L. (2016). Mechanical and thermal properties of ABS/montmorillonite nanocomposites for fused deposition modeling 3D printing. *Materials & Design*, 102: 276-283. <https://doi.org/10.1016/j.matdes.2016.04.045>
- [37] Vega, V., Clements, J., Lam, T., Abad, A., Fritz, B., Ula, N., Said, O.S. (2011). The effect of layer orientation on the mechanical properties and microstructure of a polymer. *Journal of Materials Engineering and Performance*, 20(6): 978-988. <https://doi.org/10.1007/s11665-010-9740-z>
- [38] Mahdi, H.H., Nama, S.A. (2022). Numerical investigation of free vibration for 3D printed functionally graded material cantilever beam. *International Journal on Technical and Physical Problems of Engineering*, 14(2): 27-35.
- [39] Nouman, F.E., Nama, S.A., Mahdi, H.H. (2021). Effect of infill percentage for 3D printed dies on springback for aluminum sheets. *International Journal on Technical and Physical Problems of Engineering*, 13(4): 27-32.
- [40] Hanoon, W.H., Namer, N.S.M., Nama, S.A. (2022). Bending titanium sheets with 3D-printed PETG tools. *Revue des Composites et des Matériaux Avancés-Journal of Composite and Advanced Materials*, 32(1): 39-43. <https://doi.org/10.18280/rcma.320106>
- [41] Shakir, R.A., Mezher, M.T., Robert Geber, R. (2022). Synthesis and characterization of erbium doped lead zirconate titanate thin films. *Revue des Composites et des Matériaux Avancés-Journal of Composite and Advanced Materials*, 32(3): 111-116. <https://doi.org/10.18280/rcma.320301>
- [42] Mezher, M.T., Kovács, B. (2022). An investigation of the impact of forming process parameters in single point incremental forming using experimental and numerical verification. *Periodica Polytechnica Mechanical Engineering*, 66(3): 183-196. <https://doi.org/10.1007/s00170-016-8426-6>
- [43] Mezher, M.T., Namer, N.S., Nama, S.A. (2018). Numerical and experimental investigation of using lubricant with Nano powder additives in SPIF process. *International Journal of Mechanical Engineering and Technology*, 9(13): 968-977.
- [44] Mezher, M.T., Barrak, O.S., Nama, S.A., Shakir, R.A. (2020). Predication of forming limit diagram and spring-back during SPIF process of AA1050 and DC04 sheet

- metals. *Journal of Mechanical Engineering Research and Developments*, 44(1): 337-345.
- [45] Mezher, M.T., Khazaaal, S.M., Namer, N.S.M., Shakir, R.A. (2021). A comparative analysis study of hole flanging by incremental sheet forming process of AA1060 and DC01 sheet metals. *Journal of Engineering Science and Technology*, 16(6): 4383-4403.
- [46] Mezher, M.T., Saad, M.L., Barrak O.S., Shakir, R.A. (2020). Finite element simulation and experimental analysis of nano powder additives effect in the deep drawing process. *International Journal of Mechanical & Mechatronics Engineering IJMME-IJENS*, 20(1): 166-180.
- [47] Mezher, M.T., Barrak, O.S., Namer, N.S.M. (2022). Modelling and experimental study of dissimilar arc stud welding of AISI 304L to AISI 316L stainless steel. *International Journal of Integrated Engineering*, 14(6): 88-101. <https://doi.org/10.30880/ijie.2022.14.06.009>
- [48] Mezher, M.T., Saad, M.L., Barrak, O.S., Hussein, S.K., Shakir, R.A. (2021). Multi-coupled field simulation and experimental study of AISI 316L stainless steel using resistance spot welding. *Journal of Mechanical Engineering Research and Developments*, 44(2): 150-160.
- [49] Barrak, O.S., Saad, M.L., Mezher, M.T., Hussein, S.K., Hamzah, M.M. (2019). Joining of double pre-holed aluminum alloy AA6061-T6 to polyamide PA using hot press technique. *IOP Conference Series: Materials Science and Engineering*, 881: 012062. <https://doi.org/10.1088/1757-899X/881/1/012062>
- [50] Camposeco-Negrete, C. (2020). Optimization of printing parameters in fused deposition modeling for improving part quality and process sustainability. *The International Journal of Advanced Manufacturing Technology*, 108: 2131-2147. <https://doi.org/10.1007/s00170-020-05555-9>
- [51] Zhao, Y., Chen, Y., Zhou, Y. (2019). Novel mechanical models of tensile strength and elastic property of FDM AM PLA materials: experimental and theoretical analyses. *Materials & Design*, 181: 108089. <https://doi.org/10.1016/j.matdes.2019.108089>
- [52] Verbeeten, W.M.H., Lorenzo-Bañuelos, M., Arribas-Subiñas, P.J. (2020). Anisotropic rate-dependent mechanical behavior of poly(lactic acid) processed by material extrusion additive manufacturing. *Additive Manufacturing*, 31: 100968. <https://doi.org/10.1016/j.addma.2019.100968>
- [53] Hassanifard, S., Hashemi, S.M. (2020). On the strain-life fatigue parameters of additive manufactured plastic materials through fused filament fabrication process. *Additive Manufacturing*, 32: 100973. <https://doi.org/10.1016/j.addma.2019.100973>
- [54] Ahmad, M.N., Ab Rahman, M.H., Maidin, N.A., Osman, M.H., Wahid, M.K., Mohamed Saiful Firdaus, H., Abd Aziz, N.A. (2020). Optimization on surface roughness of fused deposition modelling (FDM) 3D printed parts using Taguchi approach. *Lecture Notes in Mechanical Engineering*, 230-243. [https://doi.org/10.1007/978-981-13-9539-0\\_24](https://doi.org/10.1007/978-981-13-9539-0_24)